frontiers in Materials

ORIGINAL RESEARCH
published: 10 December 2019
doi: 10.3389/fmats.2019.00320

Investigation of the Effect of SO_2 and H_2O on VPO-Cr-PEG/TiO_2 for the Low-Temperature SCR de-NO_x

Yong Jia[1,2], Jianhua Yang[3], Jin Jiang[1], Mingyan Gu[1], Yingying Zhi[1], Lina Guo[1] and Yihua Chen[1]**

[1] School of Energy and Environment, Anhui University of Technology, Ma Anshan, China, [2] Anhui Xinchuang Energy & Environmental Protection Science & Technology Co. Ltd., Ma Anshan, China, [3] Ma'anshan Weishen Energy-Saving Environmental Protection Technology Co., Ltd., Ma Anshan, China

A catalyst 0.1VP(0.2)O-Cr(0.01)-PEG(1×10^{-4})/Ti for low-temperature SCR de-NO_x was developed and the effects of SO_2 and water vapor on its catalytic activity were investigated. Cr doping increases the molar ratio of V^{5+} to V^{4+} on the VPO catalyst, which promote oxidation of NO to NO_2 and catalytic activity of the VPO catalyst. An appropriate amount of redox-coupled V^{5+}/V^{4+} also promotes catalytic activity of the VPO catalyst. The denitration efficiency over 0.1VP(0.2)O-Cr(0.01)-PEG(1×10^{-4})/Ti was above 98% at 150–350°C. Cr doping also promotes the generation of Lewis acid around V^{5+} center and Brønsted acid (P-OH) on the VPO catalysts. The strong surface acidity of 0.1VP(0.2)O-Cr(0.01)-PEG(1×10^{-4})/Ti could restrain the adsorption of and oxidation of SO_2. Characterization (FT-IR, TG) results indicate that nearly no sulfate was deposited on the surface of 0.1VP(0.2)O-Cr(0.01)-PEG(1×10^{-4})/Ti after activity test. The competitive adsorption of water molecules and nitric oxide on the catalyst surface decreases the catalytic activity of the VPO catalyst. The addition of Cr and PEG could increase the surface area and the exposure of active site of VPO catalyst, which also increase the unoccupied active sites of VPO catalysts in the presence of water vapor. The catalyst 0.1VP(0.2)O-Cr(0.01)-PEG(1×10^{-4})/Ti for low-temperature SCR de-NO_x shows high catalytic activity and exhibits high resistance to SO_2 and water vapor.

Keywords: Cr doping, VPO, catalyst, low temperature, SCR de-NO_x

OPEN ACCESS

Edited by:
Yunfei Bu,
Nanjing University of Information Science and Technology, China

Reviewed by:
Li Yuntao,
Chongqing University of Arts and Sciences, China
Chenmin Xu,
Nanjing Normal University, China

***Correspondence:**
Lina Guo
jiayong2000@163.com;
478056296@qq.com
Yihua Chen
2398781332@qq.com

Specialty section:
This article was submitted to Energy Materials, a section of the journal Frontiers in Materials

Received: *17 September 2019*
Accepted: *21 November 2019*
Published: *10 December 2019*

Citation:
Jia Y, Yang J, Jiang J, Gu M, Zhi Y, Guo L and Chen Y (2019) Investigation of the Effect of SO_2 and H_2O on VPO-Cr-PEG/TiO_2 for the Low-Temperature SCR de-NO_x. Front. Mater. 6:320. doi: 10.3389/fmats.2019.00320

INTRODUCTION

In addition to coal-fired flue gas, industrial waste gases such as coke oven flue gas, sintering flue gas, and garbage incineration flue gas are other major sources of NO_x (Chen et al., 2015; Gamrat et al., 2016; Li et al., 2018). Among these emission sources, NO_x is discharged mainly in the form of nitric oxide (NO). The selective catalytic reduction (SCR) process is currently considered to be an efficient technology for controlling NO_x emissions (Niu et al., 2016; You et al., 2017). Although the V_2O_5-WO_3(MoO_3)/TiO_2 catalyst has been widely adopted as a superior catalyst for controlling NO_x in coal-fired flue gas, the highest reactive activity of V_2O_5-WO_3(MoO_3)/TiO_2 is usually at the temperature range of 300–400°C (Niu et al., 2016; You et al., 2017). However, the temperature of coke oven flue gas, sintering flue gas, and garbage incineration flue gas is below 250°C (Chen et al., 2015; Gamrat et al., 2016). The development of catalyst for low-temperature SCR denitration is extremely urgent for the control of NO_x emission from industrial flue gas.

Much effort has focused on developing catalysts for low-temperature denitration. Different metal oxides, supporters, and polymetallic catalysts have been investigated for low-temperature denitration (Andreoli et al., 2015; Stakheev et al., 2015; Cha et al., 2016; Chen et al., 2016; Wang et al., 2016). The denitration efficiency of some of these catalysts could reach more than 95% at temperature of 150°C. However, catalyst activities were generally inhibited by SO_2 and water vapor because of deposition of $(NH_4)_2SO_4$ and metal sulfates on the surface of catalyst (Cha et al., 2016; Wang et al., 2016). Accordingly, the development of low-temperature denitration catalysts with excellent SO_2 resistance and water resistance is urgent.

The surface acidity of a catalyst plays an important role in the SCR denitration process (Cha et al., 2016). The Eley-Rideal mechanism indicates that NH_3 is adsorbed on the Brønsted acid site and transforms into NH_4^+ ions (Yu et al., 2016). This species reacts with NO to form an activated complex and then decomposes into N_2 and H_2O. SO_2 is an acidic gas, the adsorption of SO_2 on the surface of the catalyst would be restrained by increasing the surface acidity of the catalyst, which could promote the sulfation resistance of SCR catalyst. Vanadium is a widely used as a catalyst component because of its superior redox properties (Busca et al., 1998; Phil et al., 2008; Zhao et al., 2015). Vanadium phosphorus oxides (VPO), which is prepared by reacting vanadium oxides and phosphoric acid, is a type of heteropolyacid. Busca et al. investigated the oxidation of alkanes with VPO and the results show that there are abundant Brønsted acid sites (V-OH, P-OH) on the surface of VPO catalyst (Busca et al., 1986; Bond, 1991; Feng et al., 2015). Moreover, the polarization effect of the V-(O-P) bond could promote the formation of Lewis acid sites on the V^{4+} center due to the high electronegativity of P (Bond, 1991; Benziger et al., 1997).

Water vapor is another factor which degrades the catalytic performance of low-temperature denitration catalysts. Zhang et al. proposed that the competitive adsorption of water molecules and nitric oxide on the catalyst surface is responsible for the degraded catalytic performance (Zhang et al., 2014). Adsorption and desorption equilibrium of water vapor exist on catalyst surface and the proportion of active sites occupied by water molecules is constant at a certain temperature (Melánová et al., 1999). The amount of unoccupied active sites on the surface of catalysts increases as the specific surface area of the catalyst increases. Accordingly, optimizing the structure and specific surface area of the catalyst could increase its catalytic activity in the presence of water vapor.

The surface acidity and structural properties of a catalyst are closely related to its resistance to SO_2 and water vapor (Cha et al., 2016). Vanadium phosphorus oxides (VPO) have been investigated for the oxidation of alkane by several researchers because of their excellent redox properties and surface acidities (Busca et al., 1986; Bond, 1991; Benziger et al., 1997; Melánová et al., 1999; Feng et al., 2015). However, VPO catalyst has been rarely investigated for SCR denitration and the specific surface area of VPO is usually below 20 m^2/g. Bagnasco et al. reported that the layered crystalline VPO would be formed by isomorphous substitution with some trivalent metals (Al, Cr, Fe, etc.) and the surface morphology and structural properties of VPO could also be ameliorated by trivalent metals (Bagnasco et al., 1990). In this study, Cr modified VPO catalysts with titanium dioxide as the support material were prepared and polyethylene glycol (PEG) was used to improve the dispersion of active components. The low-temperature SCR denitration performance of VPO-Cr-PEG/TiO_2 and the effect of SO_2 and water vapor on catalytic activity of VPO-Cr-PEG/TiO_2 were investigated. Combining with activity test and characterization, the physicochemical properties of the VPO-Cr-PEG/TiO_2 were also investigated.

EXPERIMENTAL

Catalyst Preparation

VPO-Cr was prepared according to a liquid-phase synthesis method. Ammonium metavanadate and chromic nitrate were added to an oxalic acid solution according to a certain mole ratio and the solution was stirred for 1 h. Subsequently, the mixture was stirred for a further 2 h after adding a certain amount of phosphoric acid (85 wt.%), HCl solution(36–38 wt.%), and PEG. Thereafter, the mixture was successively evaporated at 90°C and it was transformed into wet gel. The wet gel was dried at 105°C for 4 h. Afterwards, the product was calcined at 350°C for 3 h, and the active ingredient VPO-Cr-PEG was obtained.

Using commercially available TiO_2 (specific surface area is 322 m^2/g) as support material, the VPO-Cr-PEG/TiO_2 catalyst was prepared by impregnation method. First of all, appropriate quantities of TiO_2 and VPO-Cr-PEG were added into distilled water and the mixture was stirred for 2 h. Then the mixture was evaporated in a water bath at 70°C and the solid obtained was calcined at 350°C for 3 h. The catalyst prepared at different conditions such as P/V (molar ratio of P to V, x), Cr/V (molar ratio of Cr to V, y), PEG/V (molar ratio of PEG to V, z) and the weight percentage of active ingredient (w) were denoted as wVP(x)O-Cr(y)-PEG(z)/Ti.

Catalyst Characterization

The specific surface area and average pore size were measured by a surface area analyzer (V-sorbet 2008S). The morphologies of the catalysts were examined with a scanning electron microscope (SEM) operated at 30 kV (JEOLJSM-6380LV). The chemical composition of the catalysts was analyzed by X-ray photoelectron spectroscopy (ESCALAB 250). The redox performance and NO adsorption properties of the catalysts were measured with a Chembet Pulsar TPR/TPD. The crystal structure was determined by X-ray diffraction (XD-3). Infrared spectroscopy measurements were performed with an FT-IR spectrometer (Bomen MB154S).

Activity Test

The SCR denitration activities of the VPO-Cr-PEG/TiO_2 catalysts were measured in a conventional fixed-bed reactor (inner diameter = 8 mm). The diagram of the experimental system is present in **Figure 1**.

Flue gas was simulated by mixing 0.05 vol.% NO, 0.05 vol.% NH_3, 6 vol.% O_2, 0–0.1 vol.% SO_2, and 0–16 vol.% water vapor.

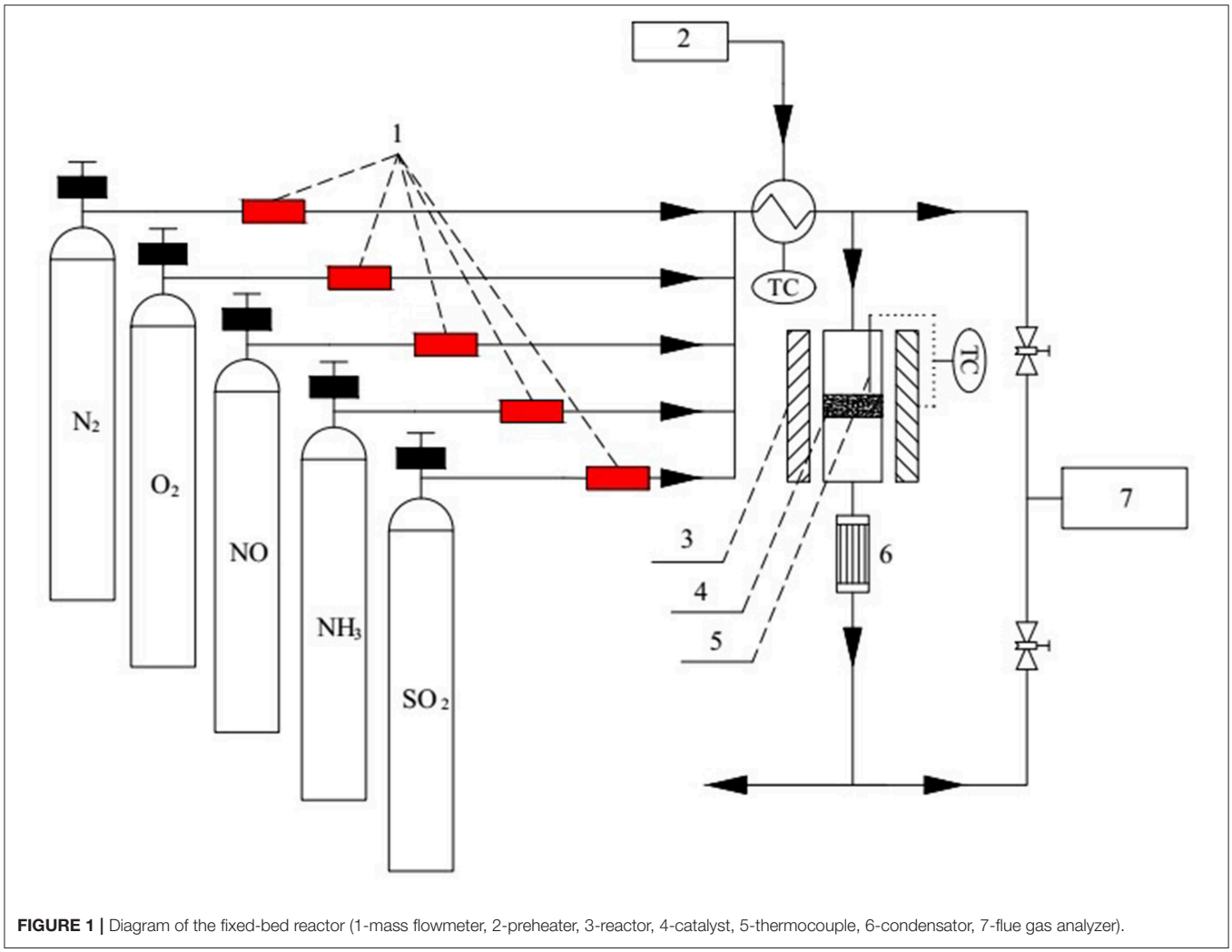

FIGURE 1 | Diagram of the fixed-bed reactor (1-mass flowmeter, 2-preheater, 3-reactor, 4-catalyst, 5-thermocouple, 6-condensator, 7-flue gas analyzer).

The mixture was balanced with N_2. The flow rate of each gas was controlled by mass flowmeter. The total gas flow rate was set to 100 mL/min and the corresponding gas hourly space velocity was about 15,000 h^{-1}. Liquid water was injected into the gas pipeline located at the center of a preheater (120°C) and it was evaporated to form water vapor. The NO_x concentration at the inlet and outlet of the fixed-bed reactor were measured with a gas analyzer (MRU Varioplus). The denitration efficiency η is expressed as:

$$\eta = (C_{in} - C_{\text{out}}) / C_{in} \times 100 \quad (1)$$

RESULTS AND DISCUSSION

SCR Denitration Activity

The NH_3-SCR deNO_x activity of the catalysts were tested at 500 ppm of NH_3, 500 ppm of NO, 6 vol.% of O_2, and 15,000 h^{-1} GHSV. The denitration efficiency of catalysts at different temperature are shown in **Figure 2**.

Obviously, the denitration efficiencies of the catalysts increase as temperature increases. The denitration efficiency of 0.1VP(0.2)O/Ti is 93% at 150°C and reaches 99.3% at temperatures above 200°C. The denitration efficiencies of Cr-PEG-modified VPO/Ti catalysts are above 98% at temperatures in the range 150–350°C. Obviously, the addition of Cr and PEG could improve the catalytic activity of VPO/Ti, especially at low reaction temperature.

Influence of SO_2 on Catalytic Activity

Selectivity of catalyst is an important parameter for SCR denitration performance. The feed gas consisted of 0.05 vol.% NO, 0.08 vol.% SO_2, 6 vol.% O_2 and balanced with N_2 was passed through catalyst, and the concentration of SO_2 and NO_x in the outlet gas were measured. Corresponding results are presented in **Figures 3**, **4**.

Figure 3 shows the outlet concentration of SO_2 and NO_x vs. time when the feed gas passed through the 0.1VP(0.2)O/Ti catalyst. The outlet concentration of SO_2 increases as time increases and it reached equilibrium and was almost the same as the inlet concentration after 40 min. Results of **Figure 3** also indicate that the outlet concentration of NO_x reached equilibrium at about 90 min.

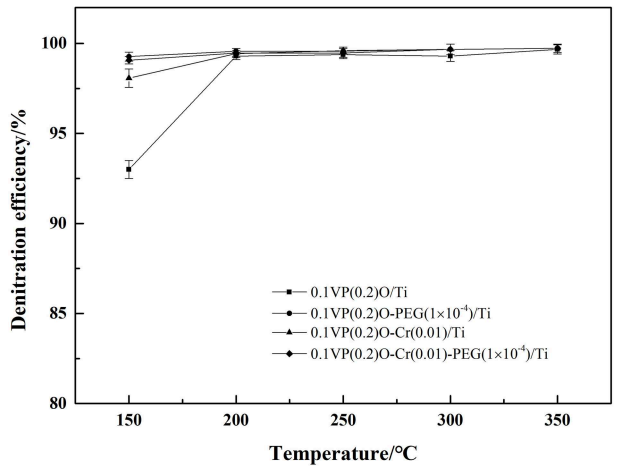

FIGURE 2 | Denitration efficiency of the supported VPO catalysts.

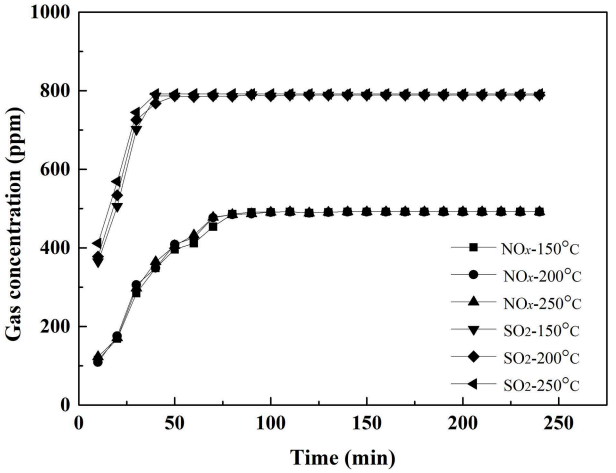

FIGURE 4 | Outlet concentration of NO_x and SO_2 vs. time over 0.1VP(0.2)O-Cr(0.01)-PEG(1 × 10^{-4})/Ti catalyst.

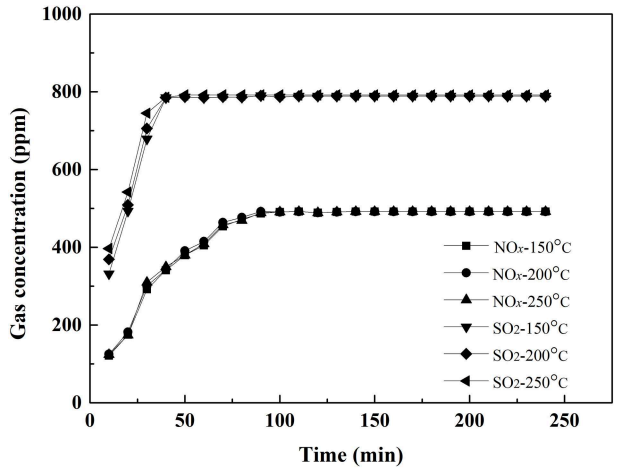

FIGURE 3 | Outlet concentration of NO_x and SO_2 vs. time over 0.1VP(0.2)O/Ti catalyst.

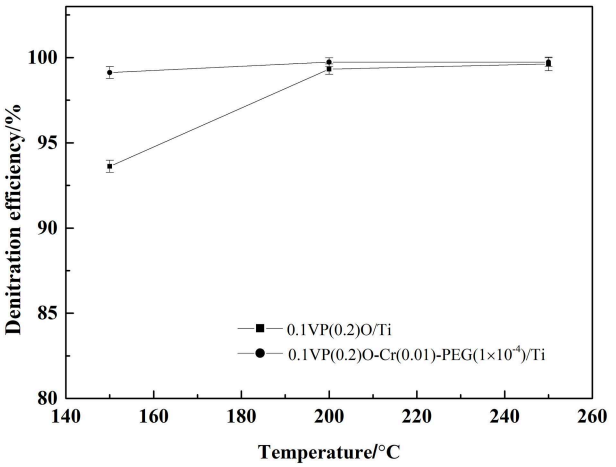

FIGURE 5 | Denitration efficiency of catalysts after SO_2 treatment.

Figure 4 shows the outlet concentration of SO_2 and NO_x vs. time when the feed gas passed through the 0.1VP(0.2)O-Cr(0.01)-PEG(1×10^{-4})/Ti catalyst. The outlet concentration of NO_x and SO_2 reached equilibrium a little faster than that of the feed gas passed through 0.1VP(0.2)O/Ti. Both results in **Figures 3**, **4** also indicate that almost no SO_2 oxidized when the feed gas passed through the VPO catalysts.

The feed gases with SO_2 mentioned above were cut off after they were in contact with catalysts for 6 h. 0.1VP(0.2)O/Ti and 0.1VP(0.2)O-Cr(0.01)-PEG(1 × 10^{-4})/Ti were then separately flushed with nitrogen (200 mL/min) for 1 h in order to remove the physically adsorbed substance. Thereafter, the NH_3-SCR deNO_x activities of the 0.1VP(0.2)O/Ti and 0.1VP(0.2)O-Cr(0.01)-PEG(1 × 10^{-4})/Ti were tested, and experimental results are shown in **Figure 5**. The experimental conditions were the same as described in *Section SCR denitration activity*. Compared with the results in **Figure 2**, the catalytic activity for SCR-deNO_x of the 0.1VP(0.2)O/Ti and 0.1VP(0.2)O-Cr(0.01)-PEG(1 × 10^{-4})/Ti in **Figure 4** did not decrease after exposure to SO_2. It indicated that the active components of 0.1VP(0.2)O/Ti and 0.1VP(0.2)O-Cr(0.01)-PEG(1 × 10^{-4})/Ti are not sulfated.

Influence of Water Vapor on Catalytic Activity

The NH_3-SCR deNO_x activity of catalysts were tested in a feed gas containing 0.05 vol.% NH_3, 0.05 vol.% NO, 6 vol.% O_2, and 4–8 vol.% water vapor. The effect of water vapor concentration on the NH_3-SCR deNO_x catalytic activity of catalysts is shown in **Figure 6**.

One can see from **Figure 6** that the denitration efficiency of 0.1VP(0.2)O/Ti decreased from 99.8 to 99.3% as water vapor concentration increased from 4 to 6 vol.%. A similar trend was

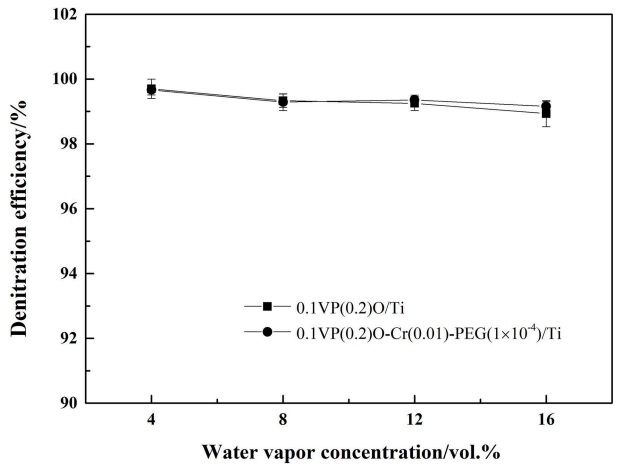

FIGURE 6 | Effect of water vapor on denitration efficiency.

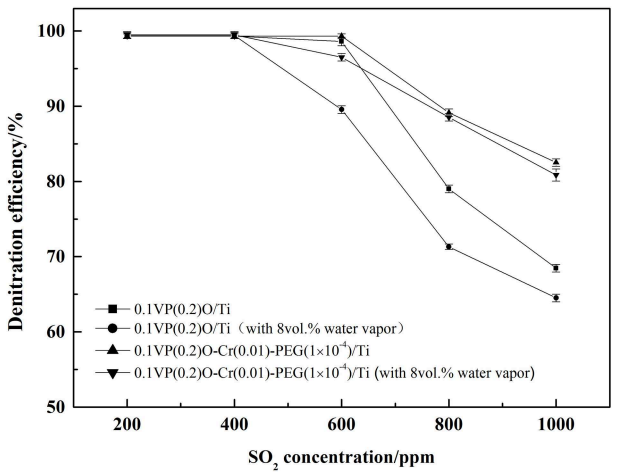

FIGURE 7 | Effect of SO_2 and water vapor on the denitration efficiency of the catalysts (200°C).

also observed for 0.1VP(0.2)O-Cr(0.01)-PEG(1×10^{-4})/Ti. One possible reason is that the number of active sites occupied by water molecules increases as the concentration of water vapor increases. As can be seen from **Figure 6**, the denitration efficiency of 0.1VP(0.2)O-Cr(0.01)-PEG(1×10^{-4})/Ti was slightly higher than that of 0.1VP(0.2)O/Ti when the water vapor concentration was above 12 vol.%. The reason may be that Cr doping ameliorate the surface and structural properties of VPO and PEG improve the dispersion of active components. There are more unoccupied active sites on surface of 0.1VP(0.2)O-Cr(0.01)-PEG(1×10^{-4})/Ti than that of 0.1VP(0.2)O/Ti in the presence of water vapor in feed gas.

Influence of Water Vapor and SO_2 on Catalytic Activity

The feed gas containing 0.05 vol.% NH_3, 0.05 vol.% NO, 6 vol.% O_2, 8 vol.% water vapor, and 0.02–0.1 vol.% SO_2 was passed through the catalysts. The effects of SO_2 and water vapor on the denitration efficiency over the 0.1VP(0.2)O/Ti and 0.1VP(0.2)O-Cr(0.01)-PEG(1×10^{-4})/Ti were investigated and results are presented in **Figure 7**. It can be seen from **Figure 7** that the catalytic activity did not decrease when the SO_2 concentration was below 400 ppm. As SO_2 concentration increased from 400 to 1,000 ppm, the denitration efficiency over 0.1VP(0.2)O/Ti decreased from 99.4 to 64.5% and the denitration efficiency over 0.1VP(0.2)O-Cr(0.01)-PEG(1×10^{-4})/Ti descreased from 99.7 to 81%. Obviously, the Cr-PEG-modified VPO/Ti catalyst has higher catalytic activity than the VPO/Ti catalyst in the presence of SO_2 and water vapor.

The sulfation of active components and the surface deposition of ammonium sulfate of catalysts are the primary reason for the decline of the NH_3-SCR deNO_x catalytic activity in the presence of SO_2 and water vapor (Cha et al., 2016; Chen et al., 2016; Wang et al., 2016).

SO_2 and water vapor were removed from the feed gas and the denitration efficiency was measured over time. These

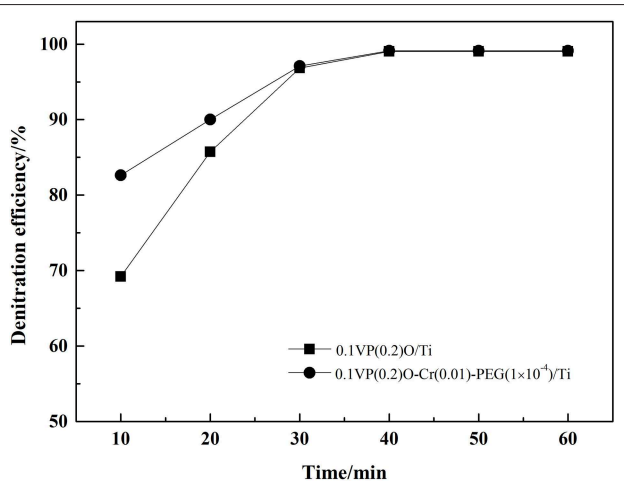

FIGURE 8 | Denitration efficiency of catalyst after remove SO_2 and water vapor in feed gas.

corresponding results are shown in **Figure 8**. Obviously, the denitration efficiency of both the 0.1VP(0.2)O/Ti and 0.1VP(0.2)O-Cr(0.01)-PEG(1×10^{-4})/Ti catalysts gradually recovered to the level observed when SO_2 was absent from the feed gas after 40 min. It could be concluded that the decreased catalytic activity of 0.1VP(0.2)O/Ti and 0.1VP(0.2)O-Cr(0.01)-PEG(1×10^{-4})/Ti was not due to the sulfation of active components and the surface deposition of ammonium sulfate, because the sulfation of active components is irreversible and the decomposition temperature of ammonium sulfate is about 280°C.

The reason for these experimental results may be that parts of ammonia react with SO_2 and water vapor in the stainless steel tube located between preheater and reactor. Accordingly, the amount of ammonia reacted with NO_x in the reactor is

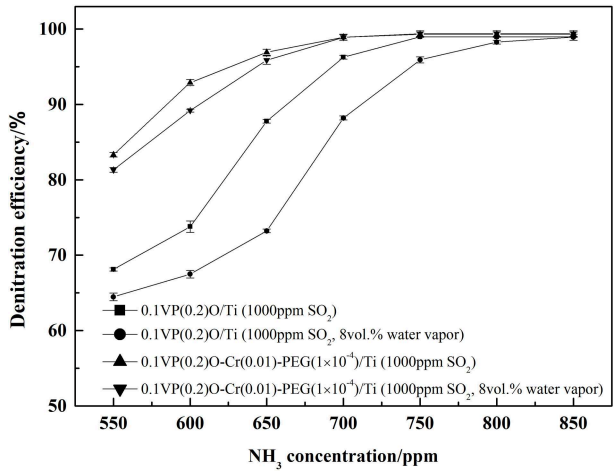

FIGURE 9 | Effect of NH_3 concentration on the denitration efficiency in the presence of SO_2 and water vapor.

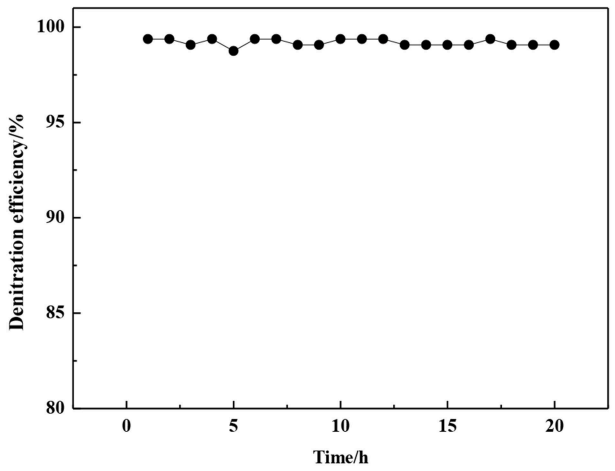

FIGURE 10 | Effects of SO_2 and water vapor on denitration efficiency of 0.1VP(0.2)O-Cr(0.01)-PEG(1×10^{-4})/Ti catalyst.

insufficient, which lead to the decrease of denitration efficiency. If this is the case, the denitration efficiency would increase as the ammonia concentration increases. Keeping the concentration of other gas constant as the situation presented in **Figure 7**, the denitration efficiency vs. NH_3 concentration was tested with SO_2 and water vapor in the feed gas, and corresponding results are present in **Figure 9**. Obviously, the denitration efficiency increases as NH_3 concentration increases with SO_2 and water vapor in the feed gas. When the concentration of NH_3 was above 700 ppm, the denitration efficiency over 0.1VP(0.2)O-Cr(0.01)-PEG(1×10^{-4})/Ti is almost the same as that without SO_2 and water vapor in the feed gas. The denitration efficiency of 0.1VP(0.2)O/Ti reaches 98.3% when the NH_3 concentration is above 0.08 vol.%.

In order to further confirm the above inference, the stainless steel tube between the preheater and the reactor was heated to 120°C by an electric heating belt, and the NH_3-SCR deNO_x activity of catalysts was tested in the presence of SO_2 and water vapor. The generation of ammonium sulfite in the stainless steel tube could be restrained by electric heating belt because the decomposition temperature of ammonium sulfite is about 60°C. The experimental results in **Figure 10** show that the denitration efficiency of 0.1VP(0.2)O-Cr(0.01)-PEG(1×10^{-4})/Ti is almost the same as that without SO_2 and water vapor in the feed gas. Moreover, the denitration efficiency did not decrease after 20 h of testing.

BET Surface Area of Catalysts

The BET surface areas of the VPO catalysts are displayed in **Table 1**. It can be seen from **Table 1** that Cr doping and PEG could increase the surface area of the VPO/Ti catalyst. The surface area of 0.1VP(0.2)O/Ti is about 171 m^2/g, while that of 0.1VP(0.2)O-Cr(0.01)-PEG(1×10^{-4})/Ti is about 217 m^2/g. A similar tendency was observed by Wang and Balaganapathi (Wang et al., 2003; Balaganapathi et al., 2016). PEG could reduce the surface energy during the nucleation process of the active component, which is favorable for uniform nucleation and inhibits the growth of the crystal particle. Meanwhile, PEG decomposes during the calcination of catalysts, and micropores are formed in the catalysts. Accordingly, the surface area of VPO/Ti increases by adding PEG during preparation.

TABLE 1 | BET surface area of catalysts.

Catalysts	BET surface area (m^2/g)
0.1VP(0.2)O/Ti	171
0.1VP(0.2)O-Cr(0.01)/Ti	177
0.1VP(0.2)O-PEG(1×10^{-4})/Ti	213
0.1VP(0.2)O-Cr(0.01)-PEG(1×10^{-4})/Ti	217

Competitive adsorption of water molecules and NO_x on the catalyst decreases the denitration efficiency. The adsorption-desorption balance of water vapor exists on the surface of the catalysts at any temperature. Parts of active sites on the catalyst are occupied by water vapor, which inhibits the adsorption of other reactants. Cr doping and PEG increase the surface area and the number of unoccupied active sites on the VPO catalysts in the presence of water vapor, which enhances the water vapor resistance of the VPO catalysts. The BET results are in agreement with the activity tests in *Section Influence of water vapor and SO_2 on catalytic activity*.

XPS Analysis

The chemical state and atomic concentration of elements on the surface of the catalysts were investigated by XPS. The characterization results are shown in **Figure 11** and **Table 2**. **Figure 11A** shows that the Ti*2p* spectra of both 0.1VP(0.2)O/Ti and 0.1VP(0.2)O-Cr(0.01)-PEG(1×10^{-4})/Ti could be fitted by two peaks corresponding to Ti $2p_{1/2}$ at 464.5 eV and Ti $2p_{3/2}$ at 458.8 eV (Reddy et al., 2006). The binding energy centered at 464.5 and 458.8 eV correspond to Ti^{4+}. Obviously, Cr doping and

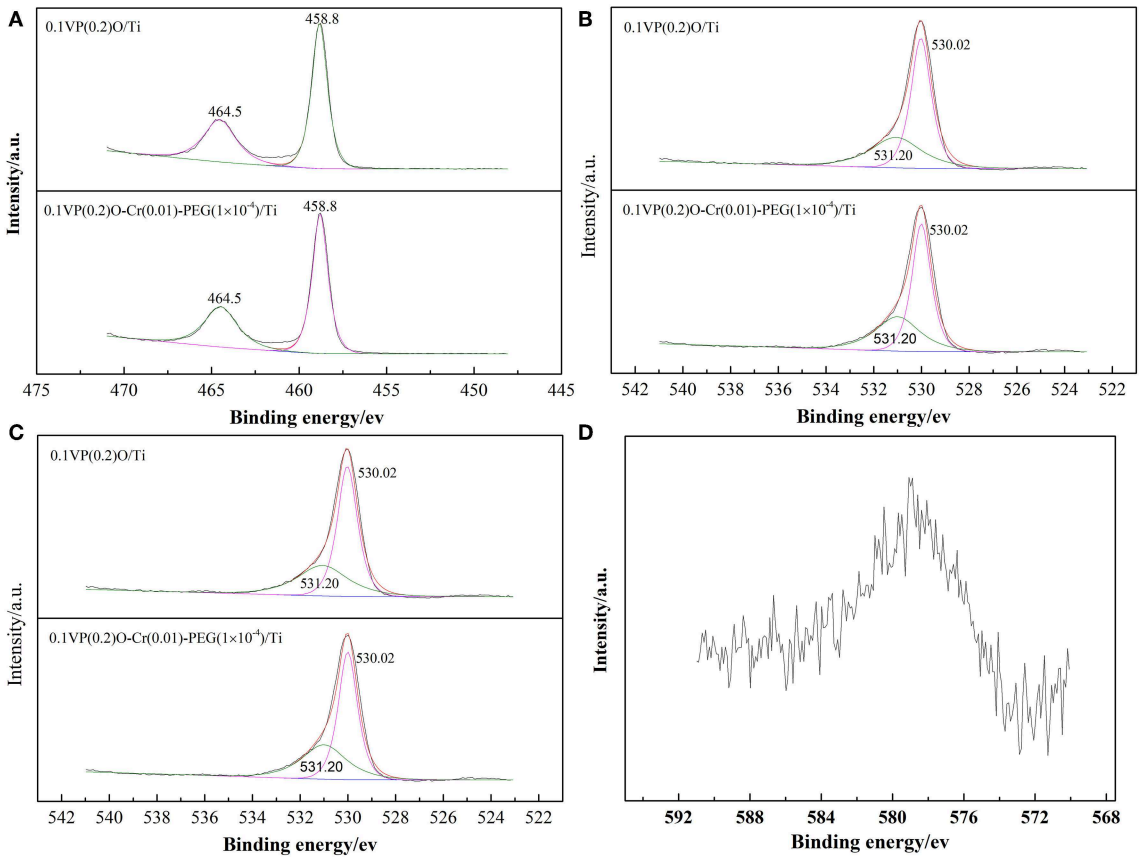

FIGURE 11 | XPS spectra of catalysts **(A)** Ti 2p **(B)** O 1s **(C)** V 2p **(D)** Cr 2P.

TABLE 2 | Element content of catalysts.

Samples	Surace atomic concentrations (%)				Surface atomic ratio		
	Ti	V	*P*	Oα	Oβ	V^{5+}/V	Oα/O
0.1VP(0.2)O/TiO_2	19.88	2.05	1.55	24.42	41.58	0.69	0.37
0.1VP(0.2)O-Cr(0.01)-PEG(1×10^{-4})/Ti	19.43	2.09	1.69	24.12	41.06	0.73	0.37

PEG have little effect on the binding energy of Ti $2p_{1/2}$ and Ti $2p_{3/2}$ in the 0.1VP(0.2)O/Ti catalyst.

Figure 11B indicates that the overlapped O *1s* peak could be fitted by two peaks at 530.02 and 531.2 eV, which represent lattice oxygen O_β and surface chemisorbed oxygen O_α, respectively (Larachi et al., 2002). Obviously, the binding energies of O_β and O_α on the surface of 0.1VP(0.2)O-Cr(0.01)-PEG(1×10^{-4})/Ti is almost the same as that of 0.1VP(0.2)O/Ti. Moreover, the relative fractions of O_α in 0.1VP(0.2)O/Ti and 0.1VP(0.2)O-Cr(0.01)-PEG(1×10^{-4})/Ti are about 0.37.

Figure 11C shows the V *2p* XPS spectra of 0.1VP(0.2)O/Ti and 0.1VP(0.2)O-Cr(0.01)-PEG(1×10^{-4})/Ti. The binding energies centered at 517.25 and 516.25 eV correspond to V^{5+} and V^{4+}, respectively (Abon and Volta, 1997; Bayati et al., 2010). Although the binding energy of 0.1VP(0.2)O/Ti showed almost no shift after Cr doping, the molar ratio of V^{5+} to V^{4+} in 0.1VP(0.2)O-Cr(0.01)-PEG(1×10^{-4})/Ti is higher than that of 0.1VP(0.2)O/Ti. The relative percentage of V^{5+} is 0.69 in 0.1VP(0.2)O/Ti and 0.73 in 0.1VP(0.2)O-Cr(0.01)-PEG(1×10^{-4})/Ti. Cr doping promotes the formation of V^{5+} ($VOPO_4$) and the oxidation of NO to NO_2, which is favorable for low-temperature SCR activity (Volta, 2001; Taufiq-Yap et al., 2010). An appropriate amount of redox-coupled V^{5+} and V^{4+} also promotes the catalytic activity of the VPO catalyst (Centi, 1993; Stakheev et al., 2015; Ren et al., 2016; Salazar et al., 2016).

Figure 11D shows the Cr *2p* XPS spectra of 0.1VP(0.2)O-Cr(0.01)-PEG(1×10^{-4})/Ti. The overlapped peaks at 576–580 eV could be assigned to Cr (Ren et al., 2016). The mixed peaks in **Figure 11D** are difficult to deconvolute, as the Cr content is relatively low.

NH_3-IR Analysis

FT-IR spectroscopy was used to analyze the surface acidity of 0.1VP(0.2)O/Ti and 0.1VP(0.2)O-Cr(0.01)-PEG(1×10^{-4})/Ti due to ammonia adsorption. **Figure 12** shows the spectrum of the adsorbed NH_3 species on the surface of the two catalysts.

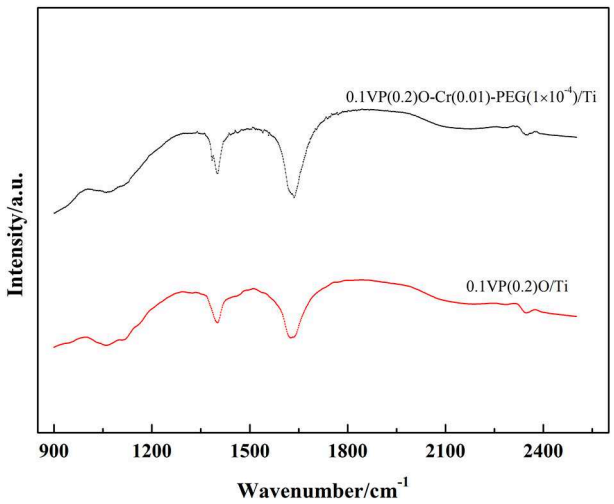

FIGURE 12 | NH_3-IR spectra of catalysts.

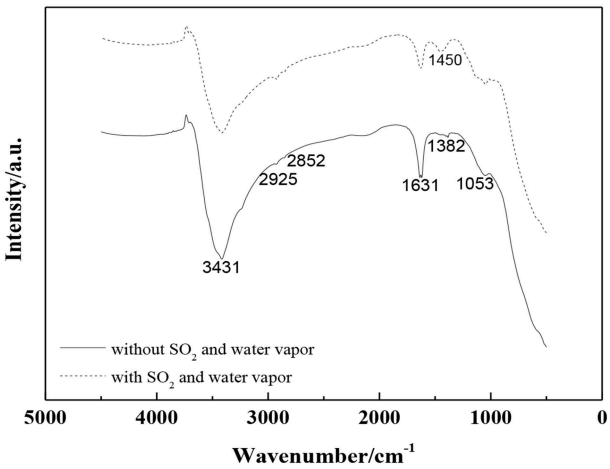

FIGURE 13 | FT-IR spectra of catalyst.

The band centered at 1,401 cm^{-1} is ascribed to N-H bending vibrations in chemisorbed NH_3 on Brønsted acid sites, while the bands centered at 1,619 cm^{-1} are assigned to NH_4^+ on Lewis acid sites.

As **Figure 12** shows, the addition of PEG and Cr to VPO/Ti could strengthen the intensity of the Brønsted acid sites and Lewis acid sites. This could be explained as follows: as the surface area of 0.1VP(0.2)O/Ti increases by adding PEG and Cr, the number of exposed surface acid sites also increases. Meanwhile, Cr doping leads to phosphorus deposition on the surface of 0.1VP(0.2)O-Cr(0.01)-PEG(1×10^{-4})/Ti, which could promote the formation of a Brønsted acid (P-OH). Moreover, the addition of Cr in VPO/Ti could increase the amount of V^{5+} and Lewis acid sites. A similar tendency was also observed by Pierini (Pierini and Lombardo, 2005a,b).

Brønsted acid sites on the catalyst are widely recognized as active sites for NH_3-SCR deNO_x. The NH_3-IR results in **Figure 12** are in good agreement with the activity tests in **Figure 2**. Furthermore, 0.1VP(0.2)O-Cr(0.01)-PEG(1×10^{-4})/Ti with strong surface acidity could restrain the surface adsorption of SO_2. The NH_3-IR spectrum further confirms the experimental results in *Section Influence of SO_2 on catalytic activity* and *Section Influence of water vapor and SO_2 on catalytic activity*.

FT-IR Spectra

Figure 13 shows the FTIR spectra of 0.1VP(0.2)O-Cr(0.01)-PEG(1×10^{-4})/Ti with/without SO_2 and water vapor in the feed gas after the activity test. The characteristic peak centered at 502 cm^{-1} is attributed to symmetric stretching vibrations in TiO_2. The band at around 1,053 cm^{-1} is ascribed to asymmetric stretching vibrations of $V^{5+} = O$. The band at 1,382 cm^{-1} is attributed to nitrate. The bands around 1,450, 1,631, and 3,432 cm^{-1} could be attributed to NH_3, an -OH group, and H_2O, respectively. The bands centered at 2,852 and 2,923 cm^{-1} are ascribed to symmetric stretching and asymmetric stretching vibrations in methylene, respectively. Obviously, nearly no difference was observed in the FT-IR spectra for 0.1VP(0.2)O-Cr(0.01)-PEG(1×10^{-4})/Ti after activity test with/without SO_2 and water vapor in feed gas. Moreover, the FT-IR spectra also indicate that no sulfate formed on the surface of catalyst after the activity test. The 0.1VP(0.2)O-Cr(0.01)-PEG(1×10^{-4})/Ti shows excellent resistance to SO_2 and water vapor (**Figure 10**), which is further confirmed by the FT-IR spectra.

Thermogravimetric Analysis (TG)

The TG curves of 0.1VP(0.2)O-Cr(0.01)-PEG(1×10^{-4})/Ti before and after the activity test with SO_2 and water vapor in the feed gas were present in **Figure 14**. Obviously, water is lost in the temperature range 25–90°C before and after the activity test. **Figure 14** The bound water linked to phosphate groups is lost in the temperature range 70–130°C, and that linked to Cr^{3+} and VO^{3+} is lost between 150 and 250°C. Furthermore, mass was lost in the 300–620°C temperature range for both catalysts. This loss could be ascribed to water being coordinated to Cr in the catalysts.

Compared to the 0.1VP(0.2)O-Cr(0.01)-PEG(1×10^{-4})/Ti catalyst before the activity test, no accelerated mass loss in the range 200–400°C was observed in the TG curves for the 0.1VP(0.2)O-Cr(0.01)-PEG(1×10^{-4})/Ti catalyst after the activity test. Ammonium sulfate decomposes at a temperature of 230°C, and ammonium bisulfate decomposes at a temperature of 350°C. The TG results further confirmed that there are no ammonium sulfate and ammonium bisulfate deposited on the 0.1VP(0.2)O-Cr(0.01)-PEG(1×10^{-4})/Ti, which is consistent with the FTIR results shown in **Figure 10**. This could be explained as follows: SO_2 adsorption on the surface of 0.1VP(0.2)O-Cr(0.01)-PEG(1×10^{-4})/Ti was restrained because of the strong surface acidity of catalysts. Meanwhile, SO_2 is hardly to be oxidize to SO_3 in the gas phase without catalyst. The ammonium sulfite generated by reaction of SO_2 with NH_3 is thermally unstable at a reaction temperature of 200°C.

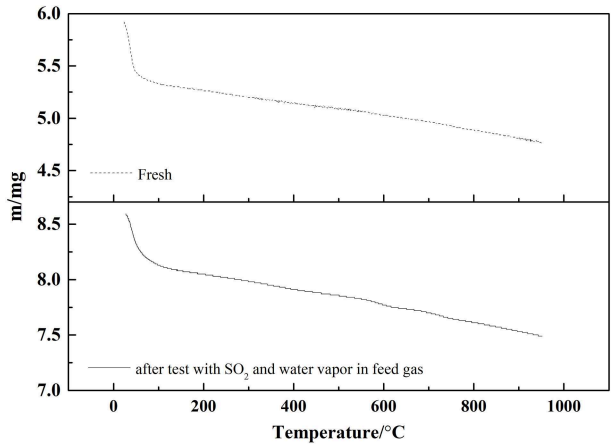

FIGURE 14 | TG curve of catalyst before and after test.

CONCLUSION

A low-temperature SCR de-NO_x catalyst 0.1VP(0.2)O-Cr(0.01)-PEG(1×10^{-4})/Ti was developed and the effects of SO_2 and water vapor on the catalytic activity of catalyst were investigated. The activity test results show that the denitration efficiency over 0.1VP(0.2)O-Cr(0.01)-PEG(1×10^{-4})/Ti was above 98% at temperatures in the range 150–350°C. Cr doping increases the molar ratio of V^{5+} to V^{4+} on the VPO catalyst, which promote oxidation of NO to NO_2 and catalytic activity of the VPO catalyst. An appropriate amount of redox-coupled V^{5+}/V^{4+} promotes the catalytic activity of the VPO catalyst. The addition of Cr increases Brønsted acid (P-OH) and Lewis acid sites around V^{5+} on the VPO catalysts. The NH_3-IR spectra show that the intensity of the Brønsted acid (P-OH, V-OH) and Lewis acid of the VPO catalyst increases after Cr doping. 0.1VP(0.2)O-Cr(0.01)-PEG(1×10^{-4})/Ti catalyst with strong surface acidity could restrain the SO_2 adsorption and the oxidation of SO_2 on the catalyst. SO_2 had little effect on the catalytic activity of 0.1VP(0.2)O-Cr(0.01)-PEG(1×10^{-4})/Ti. Characterization (FTIR, TG) results indicate that there was no ammonium sulfate deposited on the surface of 0.1VP(0.2)O-Cr(0.01)-PEG(1×10^{-4})/Ti and the active components of 0.1VP(0.2)O-Cr(0.01)-PEG(1×10^{-4})/Ti were not sulfated in the presence of SO_2 in feed gas. Generally, competitive adsorption of water molecules and reactant on the active site decreases the catalytic activity of low temperature NH_3-SCR denitration catalyst. The addition of Cr and PEG increase the surface area and the unoccupied active sites in the VPO catalysts in the presence of water vapor, which enhance the water vapor resistance of the VPO catalysts. The low-temperature SCR deNO_x catalyst 0.1VP(0.2)O-Cr(0.01)-PEG(1×10^{-4})/Ti shows high catalytic activity and exhibits good resistance to SO_2 and water vapor.

DATA AVAILABILITY STATEMENT

All datasets generated for this study are included in the article/supplementary material.

AUTHOR CONTRIBUTIONS

YJ, JJ, and JY was mainly responsible for the preparation and testing of catalysts. LG is mainly responsible for the characterization of catalysts. MG, YZ, and YC put forward their opinions on the grammar and structure of the whole paper.

FUNDING

This work was financially supported by the Major National R&D projects of China (2017YFB0601805) and Natural Science Foundation for the Higher Education Institutions of Anhui Province of China (KJ2019A0079).

REFERENCES

Abon, M., and Volta, J. C. (1997). Vanadium phosphorus oxides for N-butane oxidation to maleic anhydride. *Appl. Catal. A Gen.* 157, 173–193. doi: 10.1016/S0926-860X(97)00016-1

Andreoli, S., Deorsola, F. A., Galletti, C., and Pirone, R. (2015). Nanostructured MnO_x catalysts for low-temperature NO_x SCR. *Chem. Eng. J.* 278, 174–182. doi: 10.1016/j.cej.2014.11.023

Bagnasco, G., Ciambelli, P., Ginestra, A. L., and Turco, M. (1990). Determination of the surface acidity of layered metal phosphates by NH_3 temperature-programmed desorption. *Thermoch. Acta* 162, 91–97. doi: 10.1016/0040-6031(90)80330-2

Balaganapathi, T., Kaniamuthan, B., and Vinoth, S. (2016). PEG assisted synthesis of porous TiO_2 using sol-gel processing and its characterization studies. *Mater. Chem. Phys.* 189, 50–55. doi: 10.1016/j.matchemphys.2016.12.016

Bayati, M. R., Golestani-Fard, F., and Moshfegh, A. Z. (2010). Photo-degradation of methelyne blue over V_2O_5 –TiO_2, nano-porous layers synthesized by micro arc oxidation. *Catal. Lett.* 134, 162–168. doi: 10.1007/s10562-009-0231-5

Benziger, J. B., Guliants, V., and Sundaresan, S. (1997).New precursor to vanadium phosphorus oxide catalysts. *Catal. Today* 33, 49–56. doi: 10.1016/S0920-5861(96)00135-6

Bond, G. C. (1991). Vanadium oxide monolayer catalysts preparation, characterization and catalytic activity. *Appl. Catal.* 71, 1–31. doi: 10.1016/0166-9834(91)85002-D

Busca, G., Centi, G., Trifirò, F., and Lorenzelli, V. (1986). Surface acidity of vanadyl pyrophosphate, active phase in n-butane selective oxidation. *J. Phys. Chem.* 90, 1337–1344. doi: 10.1021/j100398a026

Busca, G., Lietti, L., Ramis, G., and Berti, F. (1998). Chemical and mechanistic aspects of the selective catalytic reduction of NO_x, by ammonia over oxide catalysts: a review. *Appl. Catal. B Environ.* 18, 1–36. doi: 10.1016/S0926-3373(98)00040-X

Centi, G. (1993).Vanadyl pyrophosphate - a critical overview. *Catal. Today* 16, 5–26. doi: 10.1016/0920-5861(93)85002-H

Cha, W., Ehrman, S. H., and Jurng, J. (2016). CeO_2 added V_2O_5/TiO_2 catalyst prepared by chemical vapor condensation (CVC) and impregnation method for enhanced NH_3-SCR of NO_x at low temperature. *J. Environ. Chem. Eng.* 4, 556–563. doi: 10.1016/j.jece.2015.10.033

Chen, W. S., Luo, J., Qin, L. B., and Han, J. (2015).Selective autocatalytic reduction of NO from sintering flue gas by the hot sintered ore in the presence of NH_3. *J. Environ. Manage.* 164, 146–150. doi: 10.1016/j.jenvman.2015.09.001

Chen, Y., Zhang, Z. T., Liu, L. L., Mi, L., and Wang, X. D. (2016). *In situ* DRIFTS studies on MnO_x nanowires supported by activated semi-coke for low

temperature selective catalytic reduction of NO_x with NH_3. *Appl. Surf. Sci.* 366, 139–147. doi: 10.1016/j.apsusc.2016.01.052

Feng, X. Z., Yao, Y., Su, Q., Zhao, L., and Jiang, W. (2015).Vanadium pyrophosphate oxides: the role of preparation chemistry in determining renewable acrolein production from glycerol dehydration. *Appl. Catal. B Environ.* 164, 31–39. doi: 10.1016/j.apcatb.2014.08.049

Gamrat, S., Poraj, J., Bodys, J., Smolka, J., and Adamczyk, W. (2016). Influence of external flue gas recirculation on gas combustion in a coke oven heating system. *Fuel. Process. Technol.* 152, 430–437. doi: 10.1016/j.fuproc.2016.07.010

Larachi, F., Pierre, J., Adnot, A., and Bernis, A. (2002). Ce 3d XPS study of composite Cex Mn1-xO2-y wet oxidation catalysts. *Appl. Surf. Sci.* 195, 236–250. doi: 10.1016/S0169-4332(02)00559-7

Li, X., Zhang, C., Zhang, X. P., Li, W., Tan, P., Ma, L., et al. (2018). Study on improving the SO_2 tolerance of low-temperature SCR catalysts using zeolite membranes: NO/SO_2 separation performance of aluminogermanate membranes. *Chem. Eng. J.* 335, 483–490. doi: 10.1016/j.cej.2017.10.184

Melánová, K., Beneš, L., VlcEk, M., Patrono, P., and Massucci, M. A. (1999). Preparation and characterization of vanadyl phosphates modified with two trivalent metal cations. *Mater. Res.* 34, 895–903. doi: 10.1016/S0025-5408(99)00086-0

Niu, Y. Q., Shang, T., Hui, S., Zhang, X. L., Lei, Y., Lv, Y., and Wang, S. (2016). Synergistic removal of NO and N_2O in low temperature SCR process with MnOx/Ti based catalyst doped with Ce and V. *Fuel* 185, 316–322. doi: 10.1016/j.fuel.2016.07.122

Phil, H. H., Reddy, M. P., Kumar, P. A., Ju, L. K., and Hyo, J. S. (2008). SO_2 resistant antimony promoted V_2O_5/TiO_2 catalyst for NH_3-SCR of NO_x at low temperatures. *Appl. Catal. B Environ.* 78, 301–308. doi: 10.1016/j.apcatb.2007.09.012

Pierini, B. T., and Lombardo, E. A. (2005a). Structure and properties of Cr promoted VPO catalysts. *Mater. Chem. Phys.* 92, 197–204. doi: 10.1016/j.matchemphys.2005.01.009

Pierini,. B. T., and Lombardo, E. A. (2005b). Cr, Mo and W used as VPO promoters in the partial oxidation of n-butane to maleic anhydride. *Catal. Today* 107, 323–329. doi: 10.1016/j.cattod.2005.07.084

Reddy, B. M., Rao, K. N., and Reddy, G. K. (2006). Characterization and catalytic activity of V_2O_5/Al_2O_3-TiO_2 for selective oxidation of 4-methylanisole. *J. Mol. Catal. A Chem.* 253, 44–51. doi: 10.1016/j.molcata.2006.03.016

Ren, Z., Xu, X., Wang, X., Gao, B., and Yue, Q. (2016). FTIR, Raman, and XPS analysis during phosphate, nitrate and Cr(VI) removal by amine cross-linking biosorbent. *J. Colloid Interface Sci.* 468, 313–323. doi: 10.1016/j.jcis.2016.01.079

Salazar, M., Hoffmann, S., Singer, V., Becker, R., and Grünert, W. (2016). Hybrid catalysts for the selective catalytic reduction (SCR) of NO by NH3. On the role of fast SCR in the reaction network. *Appl. Catal. B Environ.* 199, 433–438. doi: 10.1016/j.apcatb.2016.06.043

Stakheev, A. Y., Mytareva, A. I., Bokarev, D. A., Baeva, G. N., and Krivoruchenko, D. S. (2015). Combined catalytic systems for enhanced low-temperature NO x, abatement. *Catal. Today* 258, 183–189. doi: 10.1016/j.cattod.2015.05.023

Taufiq-Yap, Y. H., Theam, K. L., and Hutchings, G. J. (2010). The effect of Cr, Ni, Fe, and Mn dopants on the performance of hydrothermal synthesized vanadium phosphate catalysts for n-butane oxidation. *Petrol. Sci. Technol.* 28, 997–1012. doi: 10.1080/10916460903058004

Volta, J. C. (2001). Site isolation for light hydrocarbons oxidation. *Top. Catal.* 15, 121–129. doi: 10.1023/A:1016645508285

Wang, P., Sun, H., Quan, X., and Chen, S. (2016). Enhanced catalytic activity over MIL-100(Fe) loaded ceria catalysts for the selective catalytic reduction of NO_x with NH_3 at low temperature. *J. Hazard. Mater.* 301, 512–521. doi: 10.1016/j.jhazmat.2015.09.024

Wang, X., Xu, L., Chen, X., Ji, W., and Yan, Q. (2003). Novel modifications in preparing vanadium phosphorus oxides and their applications for partial oxidation of n-butane. *J. Mol. Catal. A Chem.* 206, 261–268. doi: 10.1016/S1381-1169(03)00422-9

You, X. C., Sheng, Z. Y., Yu, D. Q., Yang, L., Xiao, X., and Wang, S. (2017). Influence of Mn/Ce ratio on the physicochemical properties and catalytic performance of graphene supported MnO_x-CeO_2 oxides for NH_3-SCR at low temperature. *Appl. Surf. Sci.* 423, 845–854. doi: 10.1016/j.apsusc.2017.06.226

Yu, C., Huang, B., Dong, L., Chen, F., and Liu, X. (2016). *In situ* FT-IR study of highly dispersed MnOx/SAPO-34 catalyst for low-temperature selective catalytic reduction of NOx by NH3. *Catal. Today* 281, 610–620. doi: 10.1016/j.cattod.2016.06.025

Zhang, M. Y., Li, C. T., and Qu, L. (2014). Catalytic oxidation of NO with O_2 over $FeMnO_x/TiO_2$: effect of iron and manganese oxides loading sequences and the catalytic mechanism study. *Appl. Surf. Sci.* 300, 58–65. doi: 10.1016/j.apsusc.2014.02.002

Zhao, X., Huang, L., Li, H. R., Hu, H., Hu, X. N., Shi, L. Y., et al. (2015). Promotional effects of zirconium doped $CeVO_4$ for the low-temperature selective catalytic reduction of NO_x with NH_3. *Appl. Catal. B Environ.* 183, 269–281. doi: 10.1016/j.apcatb.2015.10.052

Conflict of Interest: The authors declare that the research was conducted in the absence of any commercial or financial relationships that could be construed as a potential conflict of interest.